Pressure dependence of protein dynamics investigated using elastic and quasielastic neutron scattering

2005 J. Phys.: Condens. Matter 17 S3101

(http://iopscience.iop.org/0953-8984/17/40/013)

INSTITUTE OF PHYSICS PUBLISHING JOURNAL OF PHYSICS: CONDENSED MATTER

J. Phys.: Condens. Matter **17** (2005) S3101–S3109 doi:10.1088/0953-8984/17/40/013

Pressure dependence of protein dynamics investigated using elastic and quasielastic neutron scattering

A Filabozzi[1], M Di Bari[2], A Deriu[2], A Di Venere[3], C Andreani[1] and N Rosato[3]

[1] Dipartimento di Fisica and Istituto Nazionale per la Fisica della Materia, Università di Roma 'Tor Vergata', Via della Ricerca Scientifica 1, I-00133 Roma, Italy
[2] Dipartimento di Fisica and Istituto Nazionale per la Fisica della Materia, Università di Parma, Parco Area delle Scienze 7/A, I-43100 Parma, Italy
[3] Dipartimento di Medicina Sperimentale e Scienze Biochimiche and Istituto Nazionale per la Fisica della Materia, Università di Roma 'Tor Vergata', Via Montpellier 1, I-00133 Roma, Italy

E-mail: Antonio.Deriu@fis.unipr.it

Received 8 July 2005
Published 23 September 2005
Online at stacks.iop.org/JPhysCM/17/S3101

Abstract

We present here a study of the dynamics of two monomeric proteins, trypsin and lysozyme, by means of elastic and quasielastic neutron scattering under medium-to-high pressure conditions (1–1200 bar). The internal motions as probed from the average proton dynamics in the 100 ps timescale have a confined diffusive nature. On increasing the pressure up to 1200 bar the confinement volume is almost unaffected, while the fraction of protons involved is slightly decreased.

1. Introduction

Pressure is a very effective modulator of the biochemical processes: it inhibits bacterial growth, affects virus vitality, activates/inactivates enzymatic reactions. It is therefore a very useful tool for basic biophysical and biochemical studies, as well as in applied research, for instance in food technology [1].

Pressure allows the structure/function and dynamics/function relationships of proteins and protein conjugates to be analysed in detail. Macromolecular changes obtained by increasing pressure give rise to modifications of fundamental physical parameters of the protein–solvent system. High pressure can induce denaturation of monomeric proteins above 3 kbar, while in the case of multimeric proteins, dissociation can occur at lower pressure values (1–3 kbar). In the case of monomeric proteins the effects of pressure below 3 kbar can reveal important information about the flexibility and the compressibility of the system. Studies of phosphorescence lifetimes [2] and of catalytic activity [3] of various enzymes demonstrated that subtle changes in flexibility occur even at relatively low pressures (<1000 bar), i.e. far below the denaturation limit. Inhibition of biological activity at non-denaturing pressures should therefore be sought in the reduced flexibility of biological macromolecules rather

than in the dissociation- or denaturation-induced inactivation of enzymes. These phenomena are accompanied by a variation of proton mobility, and these motions can be studied at the molecular level using neutron scattering techniques. Owing to the large neutron–proton cross section, with respect to those for all the other atomic species present in a biomolecule, the neutron signal measured is essentially due to the hydrogens of the biopolymer and of hydration water. In order to minimize the signal from the latter the sample is usually fully D_2O exchanged; in this way the dominant contribution to the dynamic structure factor is due to the non-exchangeable protons of the polypeptide backbone that reflect the motions of the side chains and backbone atoms to which they are bound. Neutron incoherent elastic and quasielastic scattering experiments therefore provide useful data on the average proton mobility over scales of both time and space. In this way it is possible to extend the domain explored by other spectroscopies, like NMR and optical techniques, that give local information related to the local nature of the probe used [4–6].

We report here the results of an 'energy-resolved elastic' (ENS) and quasielastic (QENS) study on two monomeric proteins: trypsin and lysozyme. Previous studies demonstrated that they both show variations of catalytic activity with pressure well below the denaturation threshold (above 3000 bar): the trypsin catalytic rate is enhanced, while lysozime is inactivated. Kinetic experiments have shown that trypsin has, in the range 1–400 bar, a negative activation volume corresponding to a pressure-induced activation, while above 400 bar the protein activity is pressure independent. This biphasic dependence has been related to its two-step enzymatic mechanism [3]. In contrast, linear dependence of catalytic rate constants on pressure, as predicted by the activated complex theory, was observed for lysozyme with a consequent enzyme inactivation [3]. This effect is also accompanied by some changes in the protein tertiary structure in the pre-denaturing range as already observed by Weber and co-workers [7].

2. Experimental details

2.1. Sample preparation

Trypsin (23.5 kDa) from bovine pancreas and lysozyme (14.4 kDa) were purchased from SIGMA. The proteins were dissolved in pure D_2O in order to exchange labile hydrogen atoms, and then lyophilized. The solution sample was then obtained by dissolving this protein powder in pure D_2O at final concentrations of 85 and 100 mg ml^{-1} (indicated as 8.5% and 10% solution in the following). In order to prevent protein from undergoing degradation, the pH value of the solution was adjusted to 3 by adding a small amount of HCl (1 mM final concentration).

In order to check for the possible occurrence of aggregation at high pressure, we have performed fluorescence measurements using 1-anilino-8-naphthalene-sulfonic acid (ANS): a fluorescent probe that increases its emission intensity upon binding non-covalently to protein hydrophobic regions. Upon aggregation the ANS fluorescence should change and depend also on the protein concentration. Steady-state fluorescence spectra were recorded on a ISS-K2 fluorometer [8]. ANS binding to the protein was detected, measuring the fluorescence emission spectra of the probe (from 400 to 550 nm) with a 350 ± 2 nm excitation wavelength. The spectra, measured at 1 bar and 1 kbar, have very similar shapes and intensities (data not shown); this indicates that no appreciable aggregation occurs with increasing pressure; some differences may occur at the level of the protein tertiary structure but they do not involve changes in the molecular weight.

2.2. Elastic and quasielastic neutron scattering

For the elastic investigation, incoherent elastic neutron temperature scans were performed on the thermal ($\lambda = 2.23$ Å) backscattering spectrometer IN13 (ILL) that provides a relatively

high Q range (up to $\widetilde{=}5$ Å^{-1}) with a good and almost Q-independent energy resolution ($\Delta E \sim 8$ μeV, FWHM). This corresponds to space and time windows of 1–6 Å and ∼100 ps respectively. In a typical temperature scan the temperature was varied in small steps from 280 to 320 K. High signal to noise ratio was obtained in 4 h per acquisition run; the elastic scattering intensities were corrected for the empty cell contribution and normalized to a slab (2 mm thick) vanadium standard.

Quasielastic neutron scattering (QENS) experiments were performed, at room temperature, on the time-of-flight spectrometer IN5 at the Institute Laue-Langevin (Grenoble, France) and on the backscattering spectrometer IRIS at the ISIS pulsed neutron source (Chilton, UK). IN5 was operated with an incident wavelength of 9 Å (energy resolution $\Delta E = 20$ μeV, FWHM) and for a range of Q from 0.04 to 1.2 Å^{-1}. For the IRIS experiment we adopted the 002 pyrolytic graphite instrument configuration that provides a range of Q from 0.4 to 1.8 Å^{-1} with an energy window from −0.25 to +1.2 meV and a resolution $\Delta E = 15$ μeV (FWHM). In both experiments raw spectra were normalized to a vanadium standard (slab shaped for IN5, cylindrical shaped for IRIS), corrected for transmission and geometry effects using standard ILL and ISIS routines. To improve the statistics the detector banks of the instruments were binned into 20 groups with an almost constant steps of Q. Long (about 24 h for both IN5 and IRIS experiments) counting times per spectrum gave very good counting statistics; this was necessary in order to take into account in the best possible way the scattering contribution from the high pressure cell, which is comparable with that of the sample. Two different pressure cells were used: (i) a cell made up from a hard aluminium alloy (ERGAL) slab (6 mm thick) with six 2 mm diameter capillary holes was produced by electro-erosion (empty cell transmission ∼90%); (ii) a second cell was made up from an array of thin-wall stainless-steel capillary tubes (inner diameter 1 mm, wall thickness 0.2 mm). The high pressure apparatus was composed of: a SITEC hand compressor for fluids, a pressure gauge, stainless-steel fittings, valves assembled in a rig that could work up to 2 kbar.

After the filling, the cell was kept closed and the pressure was checked continuously through the pressure gauge. The pressure error on the gauge is ±10 bar and the pressure has been checked to be stable within this interval throughout the time of the measurement.

2.3. Data analysis

The methodology of QENS experiments on macromolecular solutions has been discussed in detail in the literature [9, 10]. In analysing QENS data it is usually assumed that motions with markedly different timescales are decoupled; thus vibrational motions (fs timescale) are considered as independent from local diffusive motions arising from the conformational dynamics of the protein backbone (ps timescale). Their contribution is taken into account by an overall Debye–Waller factor depending on the proton mean square fluctuation $\langle u^2_{\mathrm{prot}}\rangle$. Assuming purely incoherent scattering, the dynamical structure factor of the protein, $S_{\mathrm{prot}}(Q, \omega)$, can be written as

$$S_{\mathrm{prot}}(Q, \omega) = \mathrm{e}^{-Q^2\langle u^2_{\mathrm{prot}}\rangle/3}[A_0(Q) \cdot \delta(\omega) + (1 - A_0(Q)) \cdot L_{\mathrm{prot}}(Q, \omega)]. \qquad (1)$$

The first term in the square brackets (elastic contribution) arises from the fact that the diffusion of hydrogens belonging to the protein scaffolding is confined to a limited volume: its shape and size determine the elastic incoherent scattering factor (EISF), $A_0(Q)$. The second term (quasielastic contribution) accounts for the complex time and space dependence of the conformational motions of the polypeptide backbone: mostly due to the dynamics of side chains. There is however some empirical evidence that a single-exponential decay is sufficient to provide an average description of this dynamics [11]. Therefore in the scattering law this

contribution can be represented by a single Lorentzian function $L_{\rm prot}(Q,\omega)$. Equation (1) is appropriate for the analysis of data from hydrated protein powders; in the case of protein solutions one has to also take into account the spectral broadening due to the Brownian diffusion of the molecule centre of mass, CM. This effect can be taken into account by convoluting the scattering law for the non-diffusing protein with a Lorentzian function, $L_{\rm CM}(Q,\omega)$, whose width scales with Q according to Fick's law ($\Gamma_{\rm CM}(Q) = D_{\rm CM}Q^2$) with a translational diffusion coefficient $D_{\rm CM}$ [10].

In the full scattering law we have to include the solvent contribution. Indeed, even in a fully D_2O exchanged solution, the solvent contribution is not negligible. For a 10% hydrogenous protein solution in D_2O, about 40% of the total scattering comes from the non-exchangeable protons of the protein and 60% is due to the solvent. It has been shown, both by QENS experiments and by MD simulations, that the quasielastic scattering contribution from water, at temperatures close to ambient, can be described, in a phenomenological way, with two Lorentzian components [12, 13]. One of them accounts for the fast local motions of a water molecule inside the 'cage' formed by its nearest neighbours; the second one describes the long-range translational diffusion following the relaxation of water clusters. On this basis, the contribution to the total scattering law arising from the solvent can be written as

$$S_{\rm solv}(Q,\omega) = {\rm e}^{-Q^2\langle u^2_{\rm solv}\rangle/3}[A_1(Q)\cdot L_1(Q,\omega) + (1-A_1(Q))\cdot L_2(Q,\omega)] \quad (2)$$

where the vibrational motions have been taken into account in the Debye–Waller factor, which depends on the mean square proton displacements $\langle u^2_{\rm solv}\rangle$. Here $L_1(Q,\omega)$ represents the Lorentzian component describing the first fast decay of the self-correlation function. As in pure water, we expect this component to have a width of about 2–3 meV and to be only very weakly dependent on Q. The narrower Lorentzian component, $L_2(Q,\omega)$, accounts for the long-range translation of the water centre of mass. The dependence on Q of its linewidth can be interpreted in terms of a random jump diffusion model [14]. $A_1(Q)$ is the relative weight of these Lorentzian components.

In order to model the full scattering law of our sample an instrumental flat background $B(Q)$ has to be added, together with a further elastic term (δ function) that takes into account the scattering contribution from the high pressure cell. In order to fit the data, the resulting expression for the dynamic structure factor has to be convoluted with the instrument resolution function $R(\omega)$, giving thus

$$\begin{aligned} S^{(\rm exp)}_{\rm tot}(Q,\omega) = \{&A[A_{\rm prot}(L_{\rm CM}(Q,\omega)\otimes S_{\rm prot}(Q,\omega)) \\ &+ (1-A_{\rm prot})S_{\rm solv}(Q,\omega)] + A_{\rm cell}(Q)\cdot\delta(\omega) + B(Q)\}\otimes R(\omega). \end{aligned} \quad (3)$$

In this expression A is an overall scaling factor and $A_{\rm prot}$ is the relative weight of the protein with respect to the solvent in the total scattering of the sample; it also takes into account the density changes and the corresponding change in the number of scattering centres with increasing pressure. In equation (3) several free parameters are present; in order to keep them under reasonable control, the analysis has been performed in successive steps:

(i) First, a pure solvent run was analysed. In this case $A_{\rm prot} = 0$, and from the fit we determined the cell contribution $A_{\rm cell}(Q)$ and the free parameters in the $S_{\rm solv}(Q,\omega)$ scattering function, i.e. $\langle u^2_{\rm solv}\rangle$, $A_1(Q)$ and the widths $\Gamma_1(Q)$ and $\Gamma_2(Q)$ of the two Lorentzian components in equation (2). The values of $A_1(Q)$ and of $A_{\rm cell}(Q)$ thus deduced were then kept fixed in the analysis of the spectra from the protein solutions. It is worth noticing that the values of $\Gamma_1(Q)$ and $\Gamma_2(Q)$ are, as expected, very close to the ones that could be obtained in a 'pure water' run.

(ii) A first series of preliminary fits was then performed on the sample spectra. Since the samples are 'crowded' protein solutions (concentrations around 10%) we expect values of

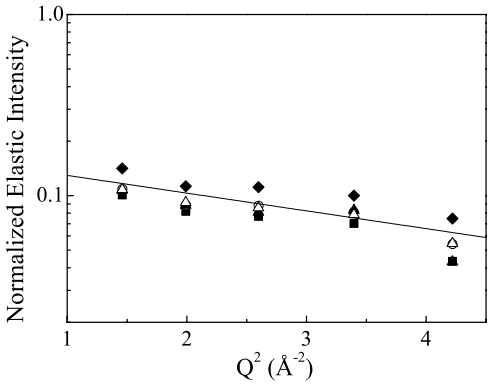

Figure 1. Q^2 dependence of the normalized elastic scattering intensity for a 10% trypsin solution in D_2O at 318 K (IN13 data). Pressures are: 1 (■), 550 (○), 750 (▲), 950 (△), 1450 (◆) bar. The mean square fluctuation reported in the text is obtained from the linear fit shown as a continuous line.

$\Gamma_1(Q)$ and $\Gamma_2(Q)$ lower than those of pure water. We decided then not to subtract a 'pure water' run from the spectra in order to avoid a systematic error in the solvent diffusivity. It is preferable to fit $S_{\rm solv}(Q, \omega)$ to equation (3) allowing $\Gamma_1(Q)$ and $\Gamma_2(Q)$ to vary in a reasonable range below their water values. The values of $\Gamma_2(Q)$ obtained in this way indicate that the solvent diffusivity is reduced by ∼10% with respect to that of pure water, due to the high solute concentration, while it is almost unchanged in the pressure range explored (up to ∼1 kbar). $\Gamma_1(Q)$ is less sensitive to solvent concentration and its values are close to those of pure water. These analyses allowed us also to check that $A_{\rm prot}$ is substantially independent of Q, with values very close to those expected on the basis of the sample concentration and isotopic composition.

(iii) In the final series of fits, $A_{\rm cell}$, $A_{\rm prot}$ and the solvent parameters ($A_1(Q)$, $\Gamma_1(Q)$ and $\Gamma_2(Q)$) were kept fixed at the values obtained in steps (i) and (ii) and only the protein parameters, A_0 and $\Gamma_{\rm prot}$, were varied. As described in the following section, it turns out that both A_0 and $\Gamma_{\rm prot}$ can be reasonably described, within the experimental accuracy, with a simple model of free diffusion inside a potential with spherical symmetry with impermeable boundaries.

3. Results and discussion

3.1. Elastic scattering

In elastic scattering experiments on IN13, the scattering contribution from solvent H nuclei is negligible because solvent and protein motions occur in quite different space–time windows [17]. The contribution of the scattering atoms of the solvent that diffuse out of the instrument space–time window is negligible and the measured elastic scattering signal is essentially due to the hydrogens of the peptide chains and of closely associated water molecules (first hydration layers).

The elastic scattering intensities were analysed in the low Q region (up to $Q \sim 2$ Å^{-1}) where the Gaussian approximation is observed: $I_{\rm el}(Q) \propto \exp[(1/3)(-Q^2\langle u^2_{\rm prot}\rangle)]$. In figure 1 $I_{\rm el}(Q)$ data for trypsin at different pressures are shown as an example. From these data we have deduced the mean square fluctuation $\langle u^2_{\rm prot}\rangle$ of protein hydrogens. Almost

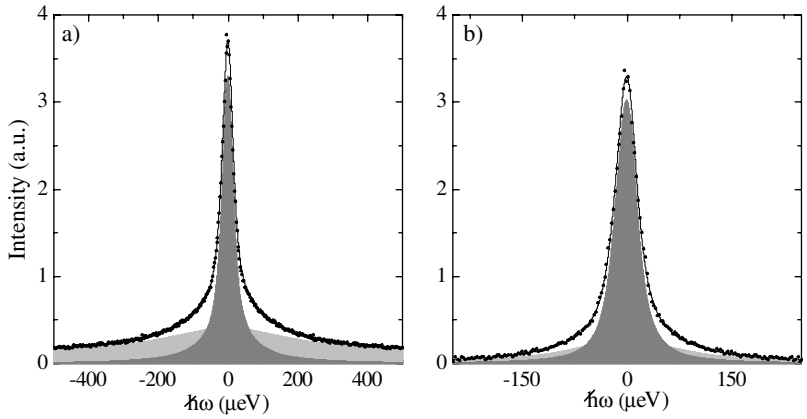

Figure 2. Quasielastic spectra at 950 bar and $Q = 1.35$ Å^{-1} for a 8.5% trypsin solution (IRIS data). (a) After subtraction of the high pressure cell contribution: the subspectra due to the protein (dark grey) and the solvent (light grey) are evident; (b) the data of panel (a) after subtraction of the solvent contribution: the elastic (dark grey) and quasielastic (light grey) protein components are evident.

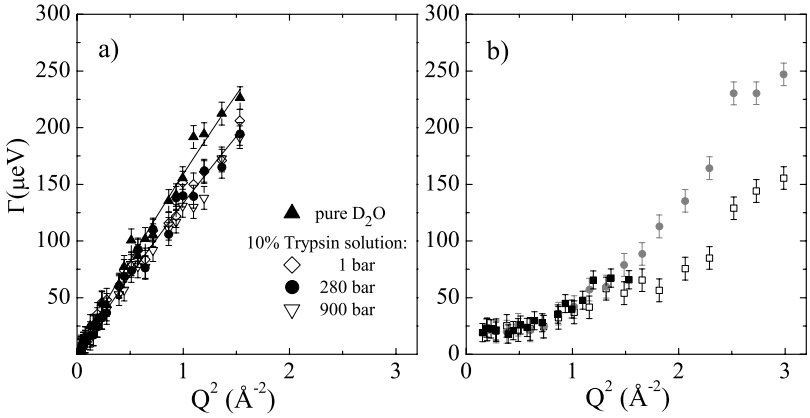

Figure 3. Q^2 dependence of the quasielastic broadenings. (a) Diffusive broadening of the narrow Lorentzian component (Γ_2 in equation (2)) of the solvent: pure water data are compared to those of a 10% trypsin solution at different pressures; (b) width of the Lorentzian component ($\Gamma_{\rm prot}$) that describes the protein conformational motions, for trypsin (■, IN5 data; □, IRIS data) and lysozyme (●, IRIS data).

no dependence of $\langle u^2_{\rm prot}\rangle$ upon pressure is detected; all the values are within one standard deviation. Therefore, within the experimental accuracy we estimate an average value for $(\langle u^2_{\rm prot}\rangle/3) = 0.23 \pm 0.04$ Å^2 from 1 to 1400 bar and in the temperature range 280–320 K. This value was then kept fixed in equation (3) when fitting the quasielastic spectra.

3.2. Quasielastic scattering: solvent dynamics

In figures 2(a) and (b) it can be seen that the spectral components due to the solvent can be reasonably separated from the protein ones owing to their different widths and Q dependences. The Q^2 dependence of the broadening of the narrow solvent component Γ_2 is shown in figure 3(a) for $p = 1$, 280 and 900 bar, together with that of pure water at 1 bar for comparison.

They have been fitted using the random jump model [14]. All the curves relating to the solvent are, as expected, systematically lower than that of pure water. The self-diffusion coefficient for the solvent is almost pressure independent and it is 15% lower than that of pure water: at $p = 900$ bar for the 8.5% solution we find $D_w = 2.2 \times 10^{-5}$ cm^2 s^{-1}. Therefore the relatively high protein concentration in the solution affects the solvent dynamics appreciably. This result also justifies our choice of including the solvent contribution in the model for the dynamic structure factor, instead of subtracting a pure solvent run. The fact that no marked pressure dependence is observed at room temperature in the solvent dynamics is not surprising. Indeed in NMR measurements on pure normal and supercooled water [18] a significant change with pressure of the translational diffusion coefficient, D_w, was observed only in the supercooled regime. The mean square fluctuation of water protons deduced from the Debye–Waller factor turns out to be $\langle u^2_{solv}\rangle^{1/2} = 0.45 \pm 0.04$ Å^{-1} in agreement with literature data on pure water [15, 16].

3.3. Quasielastic scattering: protein dynamics

As pointed out in section 2.3, the Brownian-like motion of the globular protein as a whole is explicitly taken into account. This translational motion superimposes on that of the internal conformational motions of the polypeptide chains and it turns out to be essential to obtain a satisfactory and non-ambiguous fit of the data. This is in agreement with the results of other quasielastic neutron studies on protein solutions [10] and it confirms that, in the case of small proteins, Brownian diffusion must be taken into account. This requires the knowledge of a further parameter: the protein centre of mass diffusion coefficient D_{CM}. This can be obtained from the fit of the spectra or it can be measured independently, for instance by means of dynamic light scattering. Typical D_{CM} values for small globular proteins at 1 to 5 mM solution concentration are in the range 0.5–1 $\times 10^{-6}$ cm^2 s^{-1} [19] and should therefore give rise to a small but measurable broadening in our spectra (typically between 0.2 and 0.6 times the instrumental resolution at $Q \sim 1$ Å^{-1}). In our case, from light scattering data [19] we have assumed $D_{CM} = 0.9 \times 10^{-6}$ cm^2 s^{-1} for both proteins. This value turns out to be compatible with our fits. Moreover, the expected variation of D_{CM} in the small range of concentration explored (8.5–10%) is within the experimental accuracy.

Coming now to the internal protein dynamics, from the analysis procedure described in section 2.3 we obtain: the weight of the protein contribution, A_{prot}, the elastic incoherent structure factor, EISF (A_0 in equation (1)), and the width of the quasielastic component, $\Gamma_{prot}(Q)$.

For a 10% protein solution, A_{prot} turns out to be 0.45 ($\pm$0.03) and, for the lower concentration (8.5%), 0.36 ($\pm$0.03). These values are in good agreement with the ones expected on the basis of the isotopic composition of the two samples. They were then kept fixed in the following steps of the analysis.

The conformational motions of backbone hydrogens are described with the EISF and the quasielastic width, $\Gamma_{prot}(Q)$, and both parameters indicate that in our experiments these motions are confined. In order to describe them we adopt the simple model of free diffusion inside a spherical potential with impermeable boundaries [20]. It predicts for $\Gamma_{prot}(Q)$ an asymptotic Fick-like behaviour ($\Gamma_{prot}(Q) = D_s Q^2$, D_s being the coefficient of diffusion inside the sphere) for the quasielastic broadening when $Q \gg \pi/a$, a being the radius of the confining sphere, and a constant value at low Q, i.e. when $Q < \pi/a$. From the fit of our data it turns out that $\Gamma_{prot}(Q)$ is pressure independent for both trypsin and lysozyme. We report therefore in figure 3(b) the Q^2 dependence of $\Gamma_{prot}(Q)$ for the two proteins averaged over the different pressures explored. At high values of Q, $\Gamma_{prot}(Q)$ approaches a linear Q^2 dependence from which we can estimate

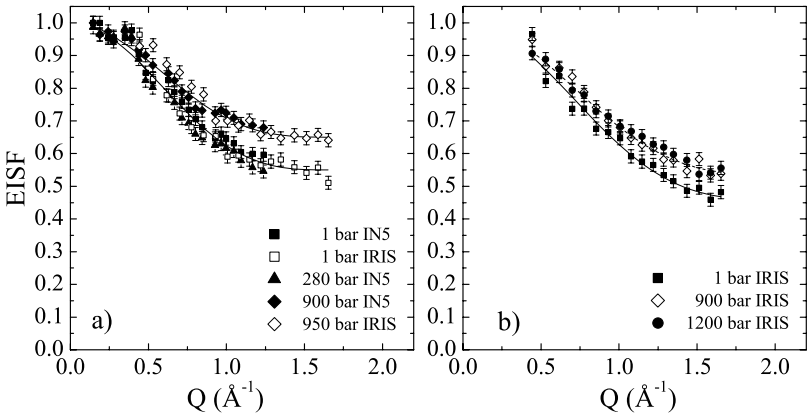

Figure 4. Q dependence of the elastic incoherent structure factor, EISF ($A_0(Q)$ in equation (1)), for the protein spectral component at different pressures; (a) trypsin; (b) lysozyme. The curves are fits to a model of free diffusion inside a sphere according to equation (4).

$D_s = 0.7 \times 10^{-5}$ cm^2 s^{-1} for trypsin and 1.0×10^{-5} cm^2 s^{-1} for lysozyme. From the plateau in the low Q region we estimate a to be around 2.5–3.0 Å. These values are confirmed in a more quantitative way from the analysis of the EISF ($A_0(Q)$ in equation (1)). The Volino and Dianoux model predicts

$$A_0(Q) = f + (1 - f)\left[\frac{3j_1(Qa)}{Qa}\right]^2 \tag{4}$$

where $j_1(Qa)$ is the first-order spherical Bessel function, a is the radius of the confining sphere and $(1 - f)$ represents the fraction of hydrogens that diffuses appreciably in the time window probed by the experiments (∼50 ps for both IN5 and IRIS).

In figures 4(a) and (b) the EISF data relating to trypsin and lysozyme are reported. It can be seen that in both cases the EISF does not change appreciably up to at least 600 bar. Around 900 bar for both proteins a small change of the f fraction is observed. For trypsin we obtain $a = (2.8 \pm 0.2)$ Å over the whole pressure range and $f = (0.55 \pm 0.02)$ from 1 bar up to 600 bar; at 900 bar, f rises to 0.66. A similar behaviour is observed for lysozyme: $a = (2.3 \pm 0.2)$ Å and $f = (0.46 \pm 0.04)$ at 1 bar rising to 0.54 at 900 bar.

These results agree with high pressure compressibility studies on trypsin by Gekko and Hasegawa [21]. They proved that the trypsin core is highly compressible due to the presence of cavities generated by imperfect packing of hydrophobic amino acid residues localized in the interior of the protein molecules. They are also in line with previous studies on several proteins where changes in mobility and flexibility were correlated [2]. Proteins with high flexibility are thermodynamically stable and, upon exposure to pressure, reduce their mobility without protein denaturation. The decrease in the population of 'more mobile' hydrogens observed above ∼900 bar demonstrates a tightening of the whole molecule that can be ascribed to the reduction of internal cavity sizes. These effects can be also correlated with the already known increased stability of the secondary structure in this pressure range; in fact the observed tightening of trypsin suggests that pressure promotes stronger intramolecular interactions, like H bonds, that follow from a close packing of the protein. On the other hand we can clearly rule out any direct relation between the changes in catalytic activity observed in the low pressure region ($p < 400$ bar) and the microscopic dynamics on the 10–100 ps timescale.

Acknowledgments

The authors wish to thank the technical staff of the neutron facilities ILL and ISIS for their support in the preparation and setting of the experiments, and the instrument scientists for the spectrometers IN13 and IN5 at ILL and IRIS at ISIS for their help in performing the experiments.

References

[1] Heremans K (ed) 1997 *High Pressure Research in Biosciences and Biotechnology* Leuven University Press
[2] Cioni P and Strambini G B 1994 *J. Mol. Biol.* **242** 291
[3] Gross M, Auerbach G and Jaenicke R 1993 *FEBS* **321** 256
[4] Mei G, Di Venere A, Malvezzi Campeggi F, Gilardi G, Rosato N, De Matteis F and Finazzi-Agro A 1999 *Eur. J. Biochem.* **265** 619
[5] Zhou J M, Zhu L, Balny C and Perrett S 2001 *Biochem. Biophys. Res. Commun.* **287** 147
[6] Sasahara K and Nitta K 1999 *Protein Sci.* **8** 1469
[7] Li T M, Hook J W III, Drickamer G and Weber G 1976 *Biochemistry* **15** 5571
[8] Paladini A A and Weber G 1981 *Rev. Sci. Instrum.* **52** 419
[9] Bée M 1988 *Quasielastic Neutron Scattering. Principles and Applications in Solid State Chemistry, Biology, and Materials Science* (Bristol: Hilger)
[10] Perez J, Zanotti J-M and Durand D 1999 *Biophys. J.* **77** 454
[11] Andreani C, Filabozzi A, Menzinger F, Desideri A, Deriu A and Di Cola D 1995 *Biophys. J.* **68** 2519
[12] Di Cola D, Deriu A, Sampoli M and Torcini A 1996 *J. Chem. Phys.* **104** 4223
[13] Di Bari M, Deriu A and Sampoli M 1999 *Physica* B **266** 92
[14] Egelstaff P A 1967 *An Introduction to the Liquid State* (New York: Academic)
[15] Teixeira J, Bellissent-Funel M-C, Chen S-H and Dianoux A J 1985 *Phys. Rev.* A **31** 1913
[16] Cavatorta F, Deriu A, Di Cola D and Middendorf H D 1994 *J. Phys.: Condens. Matter* **6** A113
[17] Tehei M, Madern D, Pfister C and Zaccai G 2001 *Proc. Natl Acad. Sci.* **98** 14356
[18] Prielmeier F X, Lang E W, Speedy R J and Lüdemann H D 1987 *Phys. Rev. Lett.* **59** 1128
[19] Tsuboi A, Izumi T, Hirata M, Xia J, Dubin P L and Kokufuta E 1996 *Langmiur* **12** 6295
[20] Volino F and Dianoux A J 1980 *Mol. Phys.* **41** 271
[21] Gekko K and Hasegawa Y 1986 *Biochemistry* **25** 6563